

ROMANIAN JOURNAL OF INFORMATION
SCIENCE AND TECHNOLOGY
Volume 20, Number 1, 2017, 18–31

A Novel Approach to Fault Classification of Power Transmission Lines Using Singular Value Decomposition and Fuzzy Reasoning Spiking Neural P Systems

Haina Rong¹, Ming Zhu², Zhipeng Feng³, Gexiang Zhang^{3,4,1,*}, Kang Huang¹

¹ School of Electrical Engineering, Southwest Jiaotong University, Chengdu, 610031, P.R. China

² Chengdu University of Information Technology, Chengdu, 610103, P.R. China

³ Robotics Research Center, Xihua University, Chengdu 610039, P.R. China

⁴ Key Laboratory of Fluid and Power Machinery (Xihua University), Ministry of Education, Chengdu 610039, P.R. China
E-mail: zhgxdylan@126.com

Abstract. A novel approach for classifying different types of faults occurring in power transmission lines is proposed by considering wavelet transform, singular value decomposition and Fuzzy Reasoning Spiking Neural P Systems (FRSNPS). In this approach, singular value decomposition in wavelet domain is used to extract features of fault current components recorded from power transmission lines; FRSNPS is applied to build the fault type classification model. Several cases with different fault types in power transmission lines are considered in the simulation experiments to verify the effectiveness of the proposed approach. The robustness to noise and to parameters of power transmission lines is also discussed.

Key-words: Membrane computing, fuzzy reasoning spiking neural P systems, fault classification, wavelet transform, singular value decomposition

1. Introduction

Membrane computing has achieved lots of theoretical results with respect to computing power equivalent to/beyond Turing and to the complexity about the use of different P

systems to solve computationally hard problems in a polynomial time [1–4]. Also, several applications [1, 5–9] were reported, many of them using spiking neural P systems (SNPS). For example, an optimization neural P system was proposed in [10] to solve well-known NP complete combinatorial optimization problems. In [11], fuzzy knowledge was represented by using SNPS. Fault section identification in power systems were addressed by using fuzzy reasoning SNPS (FRSNPS) [12–14]. These applications indicate a promising potential of SNPS to solve more real-life problems.

This work is a continuation of the previous investigations [12–14] and extends the application of FRSNPS from fault section identification to fault type classification. Fault classification is one of the most important tasks in power transmission line protection which has to be fulfilled as fast and accurate as possible to isolate the system from fault point and recover power supply after a fault occurs. Traditional techniques for fault classification often use power frequency component. They have some problems in protection speed and are susceptible to many factors such as fault types, fault resistance, fault locations and fault inception angles [15]. The recent methods for fault classification like wavelet transform [18], fuzzy logic [17] and artificial neural networks [18] mainly focused on the analysis of the transient components, which contain abundant fault information generated by faults. These methods usually require numerous training samples or their inference process is a black-box operation, which are not easily understood [19]. Therefore, fault classification deserves to be further investigated.

In this study, a novel approach is presented to classify the types of faults occurring in the power transmission lines. This approach uses wavelet transform and singular value decomposition to extract the features of fault current signals. FRSNPS is introduced to build the classification models. This is the first attempt to extend the application of FRSNPS from fault section identification to fault type classification. Extensive experiments are conducted by considering various fault conditions and parameters including fault inception angles, fault resistance and fault locations. In addition, the robustness of the introduced approach to signal-to-noise rates and variable power transmission line parameters are also discussed. Experimental results verify the feasibility, effectiveness and advantages over two methods recently reported in the literature.

2. Problem Description

A two-machine three-phase power system transmission line might encounter at least ten types of short-circuit faults: three single-phase-to-ground faults (phase A_g , B_g or C_g), three double-phase-to-ground faults (AB_g , BC_g or CA_g), three double-phase faults (AB , BC or CA) and one three-phase fault (ABC). Each fault type requires its corresponding measures to handle the fault so as to restore power supply as soon as possible. For example, when a single-phase-to-ground fault occurs, the circuit breakers (CBs) on the fault phase will trip to isolate the fault, but the CBs on sound phases will not trip; when each of the other types of faults occurs, the CBs on three phases will trip together. Thus, correct recognition of fault types can lead to proper measures, otherwise, malfunctions and rejection clips of CBs will deteriorate the effects of faults.

In summary, the fault classification problem of power transmission lines can be described

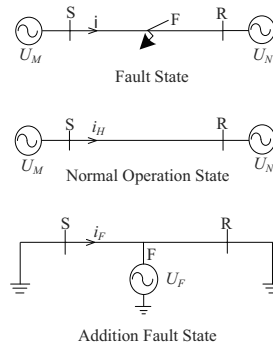


Figure 1: Transmission system states.

as follows: given the current signals through the three-phase power transmission lines, the fault types should be identified by using various techniques [20].

In this study, a novel approach is developed to classify the ten types of faults occurring in the power transmission lines by considering the combination of wavelet transform, singular value decomposition and fuzzy reasoning spiking neural P systems. The difference signals between the fault and the normal signals through the three-phase power transmission lines are first obtained; then wavelet transform is used to analyze the difference signals and further singular value decomposition is applied to extract the singular values; finally, fuzzy reasoning spiking neural P systems are employed to build the classification model to identify the fault types. The approach consists of five steps: obtaining fault current components, wavelet transform, singular value decomposition, fault classification model with FRSNPS and outputting fault types.

3. Fault Feature Extraction

As usual, a fault occurring in the transmission lines has a direct influence on the current. That is to say, the fault in the transmission lines can be identified by processing the current signals, which contain various fault information such as fault types, fault distances and fault duration time. When a fault happens in the transmission lines, the current called fault current consists of two components: load current and fault component current. The current in the normal operation state of transmission lines is load current. The fault component current in the addition fault state is caused by the fault due to the fault electrodynamic force at the fault point. A schematic illustration for the three states of transmission lines is shown in Fig. 1. According to the superposition principle [21], the fault component current i_F equals the result that the fault current i subtracts the load current i_H , namely $i_F = i - i_H$. The calculation of i_F can be performed by using the formula $i_F(t) = i(t) - i(t - nN)$, where N is the sampling number; n may be 1 or 2 because of the system frequency deviation; t represents time.

To identify the types of faults occurring in the transmission lines, fault features are extracted from the fault current. The better the features are, the more accurate the fault types are classified. In response to the characteristics of the fault current that contains sudden changes

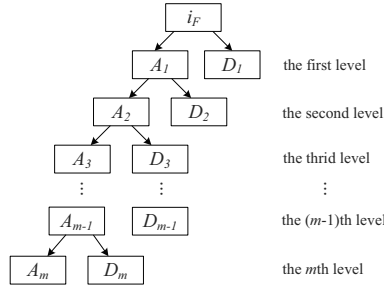


Figure 2: Wavelet transform process of the fault current signal i_F .

and abundant high frequency information, it is a good choice to use wavelet transform and singular decomposition to analyze the fault current signals. Wavelet transform is a good time-frequency analysis technique [22]. Singular value decomposition (SVD) can decrease the size of a matrix and reveal the intrinsic algebraic property of a signal by its singular values [23]. Thus, a fault current signal can be decomposed by using wavelet transform into a series of low and high frequency components at different levels. The decomposition process is shown in Fig. 2, where D_j and A_j ($j = 1, \dots, m$) represent the high and low frequency components at scale j , respectively. The frequency bands of high frequency component D_j and low frequency component A_j are listed as follows:

$$D_j : [2^{-(j+1)} f_s, 2^{-j} f_s]$$

$$A_j : [0, 2^{-(j+1)} f_s]$$

where $j = 1, \dots, m$ represents the decomposition level and f_s is the sampling rate of a signal. Thus, the wavelet coefficient matrix at scale m can be obtained from the decomposed high frequency components D_m .

Finally, SVD is used to deal with the wavelet coefficient matrix to obtain its singular value, which is called wavelet singular value in this study. Thus, the wavelet singular values, S_a, S_b, S_c and S_0 , can be obtained from the currents of three phases, A, B and C , and zero sequence phase, respectively. S_a, S_b, S_c and S_0 are normalized by $s_\varphi = S_\varphi / \max(S_a, S_b, S_c, S_0)$, where φ stands for a, b, c or 0 . Their normalized values are denoted by s_a, s_b, s_c and s_0 , respectively. Thus, s_a, s_b, s_c and s_0 will be considered as the fault features to be inputs of the subsequent classification model.

4. Fault Classification Models with FRSNPS

In this study, fuzzy reasoning spiking neural P systems with real numbers (in short r-FRSNPS) [14] are used to build the fault classification model. An rTFRSNPS of degree $m \geq 1$ is a tuple $\Pi = (O, \sigma_1, \dots, \sigma_m, \text{syn}, \text{in}, \text{out})$, where:

- (1) $O = \{a\}$ is a singleton alphabet (a is called spike);

- (2) $\sigma_1, \dots, \sigma_m$ are neurons consisting of proposition and rule neurons. Proposition neurons have the form $\sigma_i = (\theta_i, r_i), 1 \leq i \leq s$. Rule neurons have the form $\sigma_i = (\delta_i, c_i, r_i), 1 \leq i \leq t, s + t = m$, where:
- θ_i is a real number in $[0, 1]$ representing the potential value of spikes (i.e., the value of electrical impulses) contained in proposition neuron σ_i ;
 - δ_i is a real number in $[0, 1]$ representing the potential value of spikes (i.e., the value of electrical impulses) contained in rule neuron σ_i ;
 - c_i is a real number in $[0, 1]$ representing the truth value associated with rule neuron σ_i and is identical with the certainty factor of the fuzzy production rules corresponding to rule neuron σ_i ;
 - For both proposition neurons and rule neurons, r_i represents a firing (spiking) rule contained in neuron σ_i with the form $E/a^\theta \rightarrow a^\beta$, where θ and β are real numbers in $[0, 1]$, $E = \{a^n\}$ is the firing condition. The firing condition means that if and only if neuron σ_i receives at least n spikes, then the firing rule contained in the neuron can be applied, otherwise, the firing rule cannot be applied;
- (3) $syn \subseteq \{1, 2, \dots, m\} \times \{1, 2, \dots, m\}$ with $i \neq j$ for all $(i, j) \in syn, 1 \leq i, j \leq m$, is a directed graph of synapses between the linked neurons;
- (4) $in, out \subseteq \{1, 2, \dots, m\}$ indicate the input neuron set and the output neuron set of Π , respectively.

In order to present a reasoning algorithm for rFRSNPS, some parameter vectors and matrices [12–14] are described as follows:

- $\boldsymbol{\theta} = (\theta_1, \dots, \theta_s)^T$ is a real truth value vector of s proposition neurons, where θ_i ($1 \leq i \leq s$) is a real number in $[0, 1]$ representing the potential value contained in the i th proposition neuron. If there is no spike contained in a proposition neuron, its potential value is 0.
- $\boldsymbol{\delta} = (\delta_1, \dots, \delta_t)^T$ is a real truth value vector of t rule neurons, where δ_j ($1 \leq j \leq t$) is a real number $[0, 1]$ representing the potential value contained in the j th rule neuron. If there is no spike contained in a rule neuron, its potential value is 0.
- $\mathbf{C} = \text{diag}(c_1, \dots, c_t)$ is a diagonal matrix, where c_j ($1 \leq j \leq t$) is a real number in $[0, 1]$ representing the certainty factor of the j th fuzzy production rule.
- $\mathbf{D}_1 = (d_{ij})_{s \times t}$ is a synaptic matrix representing the directed connection from proposition neurons to *general* rule neurons. If there is a directed arc (synapse) from the proposition neuron σ_i to the *general* rule neuron σ_j , then $d_{ij} = 1$, otherwise, $d_{ij} = 0$.
- $\mathbf{D}_2 = (d_{ij})_{s \times t}$ is a synaptic matrix representing the directed connection from proposition neurons to *and* rule neurons. If there is a directed arc (synapse) from the proposition neuron σ_i to the *and* rule neuron σ_j , then $d_{ij} = 1$, otherwise, $d_{ij} = 0$.
- $\mathbf{E} = (e_{ji})_{t \times s}$ is a synaptic matrix representing the directed connection from rule neurons to proposition neurons. If there is a directed arc (synapse) from the rule neuron σ_j to the proposition neuron σ_i , then $e_{ji} = 1$, otherwise, $e_{ji} = 0$.

Subsequently, some multiplication operations are presented as follows.

- (1) \otimes : $D^T \otimes \theta = (\bar{d}_1, \dots, \bar{d}_t)^T$, where $\bar{d}_j = d_{1j} * \theta_1 + \dots + d_{sj} * \theta_s$, for $j = 1, \dots, t$.
- (2) \oplus : $D^T \oplus \theta = (\bar{d}_1, \dots, \bar{d}_t)^T$, where $\bar{d}_j = \min\{d_{1j} * \theta_1, \dots, d_{sj} * \theta_s\}$, for $j = 1, \dots, t$.
- (3) \odot : $D^T \odot \theta = (\bar{d}_1, \dots, \bar{d}_t)^T$, where $\bar{d}_j = \max\{d_{1j} * \theta_1, \dots, d_{sj} * \theta_s\}$, for $j = 1, \dots, t$.

In what follows, the pseudocode of the reasoning algorithm for rFRSNPS is listed as follows:

INPUT: The fuzzy truth values of the propositions corresponding to the input proposition neurons.

OUTPUT: The fuzzy truth values of the propositions corresponding to the output proposition neurons.

Step 1: Let $g = 0$ be the reasoning step;

Step 2: Set initial values of $\mathbf{D}_1, \mathbf{D}_2, \mathbf{E}, \mathbf{C}$ and the termination condition $\mathbf{O}_1 = (\text{unknown}, \dots, \text{unknown})^T$. The initial values of θ and δ are set to $\theta_g = (\theta_{1g}, \theta_{2g}, \dots, \theta_{sg})$ and $\delta_g = (\delta_{1g}, \delta_{2g}, \dots, \delta_{tg})$, respectively;

Step 3: g is increased by 1;

Step 4: The firing condition of each input neuron ($g = 1$) or each proposition neuron ($g > 1$) is evaluated. If the condition $E = a^s$ is satisfied and there is a postsynaptic rule neuron, the neuron fires and transmits a spike to the next rule neuron;

Step 5: Compute the fuzzy truth value vector δ_g according to (1);

$$\delta_g = (\mathbf{D}_1^T \otimes \theta_{g-1}) + (\mathbf{D}_2^T \oplus \theta_{g-1}) \quad (1)$$

Step 6: If $\delta_g = \mathbf{O}_1$, the algorithm halts and outputs the reasoning results;

Step 7: Evaluate the firing condition of each rule neuron. If the condition $E = a^s$ is satisfied, the rule neuron fires and transmits a spike to the next proposition neuron;

Step 8: Compute the fuzzy truth value vector θ_g according to (2). Go to Step 3.

$$\theta_g = \mathbf{E}^T \odot (\mathbf{C} \otimes \delta_g) \quad (2)$$

The normalized wavelet singular values, S_a, S_b, S_c and S_0 , are crisp and need to be fuzzified before they are used as the inputs of fault classification models based on rFRSNPS. On the basis of data analysis, two fuzzy sets are chosen for the normalized values s_a, s_b and s_c designated as **large** and **small**. Similarly, two fuzzy sets are used for the normalized value s_0 designated as **large** and **small**. The membership functions, which are shown in Fig. 3, are defined for the four normalized values according to data analysis of different fault samples. For s_a, s_b , and s_c , **small** expresses any value less than 0.5, while **large** reflects any value greater than 0.5. **small** in the functions of s_0 indicates any value less than 0.001, while **large** indicates the value greater than 0.001.

When a fault occurs in the power transmission lines, the fault component current of the fault phase has a dramatic change, while the fault component current of the sound phases slightly changes. So the wavelet singular value of a fault phase is much larger than that without any fault and the wavelet singular value of a sound phase is very small. The zero

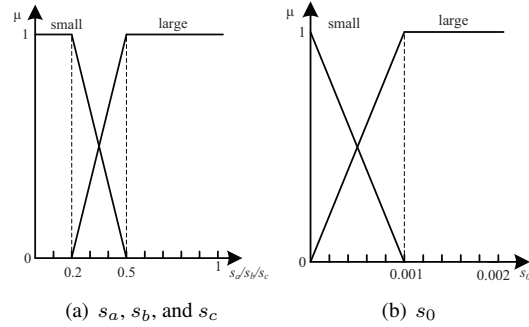


Figure 3: Fuzzy membership functions.

sequence current is theoretically zero to phase to phase faults and three phase fault. The zero sequence current is large to ground faults. Thus, the wavelet singular value of the fault component zero-sequence current to ground fault is much larger than that without any fault. The wavelet singular value of the fault component zero-sequence current of phase to phase fault is very small. Please note that **large** and **small** mentioned above are fuzzy knowledge representing transient feature values. Thus, the fuzzy production rules of fault classification are described as follows.

- R_1 : IF (s_0 is **large**) THEN (**Grounded fault**)
 R_2 : IF (s_0 is **small**) THEN (**Phase-to-Phase fault**)
 R_3 : IF (s_a is **large**) AND (s_b is **small**) AND (s_c is **small**) AND (**Grounded fault**) THEN A_g
 R_4 : IF (s_a is **small**) AND (s_b is **large**) AND (s_c is **small**) AND (**Grounded fault**) THEN B_g
 R_5 : IF (s_a is **small**) AND (s_b is **small**) AND (s_c is **large**) AND (**Grounded fault**) THEN C_g
 R_6 : IF (s_a is **large**) AND (s_b is **large**) AND (s_c is **small**) AND (**Grounded fault**) THEN AB_g
 R_7 : IF (s_a is **small**) AND (s_b is **large**) AND (s_c is **large**) AND (**Grounded fault**) THEN BC_g
 R_8 : IF (s_a is **large**) AND (s_b is **small**) AND (s_c is **large**) AND (**Grounded fault**) THEN CA_g
 R_9 : IF (s_a is **large**) AND (s_b is **large**) AND (s_c is **small**) AND (**Phase-to-Phase fault**) THEN AB
 R_{10} : IF (s_a is **small**) AND (s_b is **large**) AND (s_c is **large**) AND (**Phase-to-Phase fault**) THEN BC
 R_{11} : IF (s_a is **large**) AND (s_b is **small**) AND (s_c is **large**) AND (**Phase-to-Phase fault**) THEN CA
 R_{12} : IF (s_a is **large**) AND (s_b is **large**) AND (s_c is **large**) AND (**Phase-to-Phase fault**) THEN ABC

On the basis of fuzzy production rules, fault classification model with rFRSNPS can be built and are shown in Fig. 4, where A_l , A_s , B_l , B_s , C_l , C_s , 0_l and 0_s represent propositions “ s_a is **large**”, “ s_a is **small**”, “ s_b is **large**”, “ s_b is **small**”, “ s_c is **large**”, “ s_c is **small**”, “ s_0 is **large**”, “ s_0 is **small**”, respectively. The rFRSNPS for fault classification is described as follows:

$$\Pi_1 = (O, \sigma_1, \sigma_2, \dots, \sigma_{32}, syn, in, out)$$

where

- (1) $O = \{a\}$ is the singleton alphabet (a is called spike);
- (2) $\sigma_1, \dots, \sigma_{20}$ are proposition neurons corresponding to the propositions with fuzzy truth values $\theta_1, \dots, \theta_{20}$;
- (3) $\sigma_{21}, \dots, \sigma_{32}$ are rule neurons, where σ_{21}, σ_{22} are *general* rule neurons, $\sigma_{23}, \dots, \sigma_{32}$ are *and* rule neurons;
- (4) $syn = \{(1, 21), (2, 22), (3, 23), (3, 26), (3, 28), (3, 29), (3, 31), (3, 32), (4, 24), (4, 25), (4, 27), (4, 30), (5, 24), (5, 26), (5, 27), (5, 29), (5, 30), (5, 32), (6, 23), (6, 25), (6, 28), (6, 31), (7, 25), (7, 27), (7, 28), (7, 30), (7, 31), (7, 32), (8, 23), (8, 24), (8, 26), (8, 29), (9, 23), (9, 24), (9, 25), (9, 26), (9, 27), (9, 28), (10, 29), (10, 30), (10, 31), (10, 32), (21, 9), (22, 10), (23, 11), (24, 12), (25, 13), (26, 14), (27, 15), (28, 16), (29, 17), (30, 18), (31, 19), (32, 20)\}$;
- (5) $in = \{\sigma_1, \dots, \sigma_8\}$;
- (6) $out = \{\sigma_{11}, \dots, \sigma_{20}\}$.

5. Experiments and Analysis

The two-machine three-phase power system is simulated on PSCAD/EMTDC for producing fault samples to test the performance of the introduced approach. The Bergeron line model of PSCAD/EMTDC is considered for transmission lines. The parameters are listed as follows. Source data at sending ends: positive-sequence impedance, zero-sequence impedance and frequency are $9.19+j52.1 \Omega$, $6.69+j37.9 \Omega$ and 50 Hz, respectively; source data at receiving ends: positive-sequence impedance, zero-sequence impedance and frequency are $8.19+j42.1 \Omega$, $6.47+j33.3 \Omega$ and 50 Hz, respectively; transmission line data: length, voltage, positive-sequence impedance, zero-sequence impedance, positive-sequence capacitance and zero-sequence capacitance are 200 km, 500 kV, $3.92+j56.0 \Omega$, $36.6+j172 \Omega$, $13.5 nF/km$ and $9.20 nF/km$, respectively.

The proposed fault classification method uses only the current signals of three phases. The sampling frequency is set to 50 kHz, and the mother wavelet “db3” and 8-scaled wavelet transform are chosen. The test cases are considered for different values of fault resistance, fault location, fault inception angles [16, 24], as follows:

- (1) Fault resistance: 0, 50, 100 and 200 ohms.
- (2) Fault location: 0, 50, 100, 150 and 200 km from the bus.
- (3) Fault inception angles: 0, 30, 60, 90, 120 and 150 degrees.

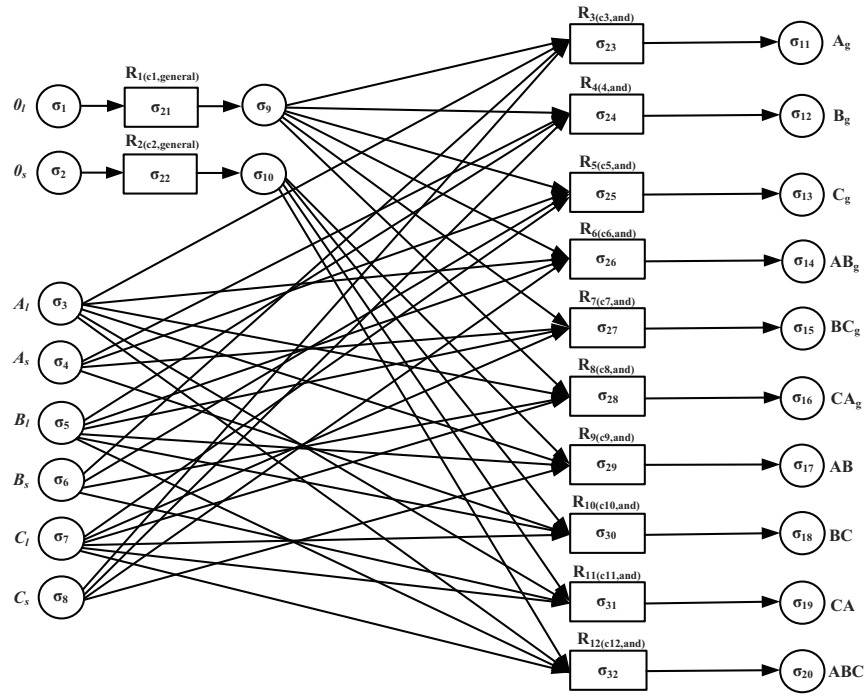


Figure 4: Fault classification models with rFRSNPS.

Table 1: Simulation conditions for four cases with different types of faults

Fault types	R_f (Ω)	Fault locations (km)	FIA ($^\circ$)
Case 1: A_g	0	50	0
Case 2: AB_g	50	100	30
Case 3: AB	100	150	60
Case 4: ABC	200	200	90

The proposed approach is tested by using 1200 independent simulations by considering different values of fault resistance, fault location and fault inception angles. Four cases for considering different types of faults are taken as examples to conduct the experiments. Their simulation conditions are given in Table 1. The classification processes for the four cases are described as follows:

Case 1: The fault is of type A_g .

We sample three phase currents with the duration 1/4 cycle after the fault inception and three phase currents with the duration 15–20 ms before the fault inception. Thus, the three phases and zero-sequence fault component currents can be calculated. Then, the wavelet singular values, 20.5098, 1.2329, 1.2341 and 7.6589 for S_a , S_b , S_c and S_0 , respectively, are obtained by using wavelet transform and SVD. The normalized feature values, 1, 0.0601, 0.0602 and 0.3734 for s_a , s_b , s_c and s_0 , respectively, are also gained. Subsequently, these

values are fuzzified by using fuzzy membership functions to get the initial states of the input proposition neurons. Finally, the reasoning algorithm is used to accomplish reasoning of fault classification.

The initial parameter matrices of the rFRSNPS for fault classification are as follows: $\theta_0=[1\ 0\ 1\ 0\ 0\ 1\ 0\ 1\ 0\ 0\ 0\ 0\ 0\ 0\ 0\ 0\ 0\ 0\ 0\ 0\ 0\ 0]$, $\delta_0=[0\ 0\ 0\ 0\ 0\ 0\ 0\ 0\ 0\ 0\ 0\ 0\ 0\ 0]$, $C=[0.95\ 0.95\ 0.95\ 0.95\ 0.95\ 0.95\ 0.95\ 0.95\ 0.95\ 0.95]$.

When $g = 1$, the results are the following: $\delta_1=[1\ 0\ 0\ 0\ 0\ 0\ 0\ 0\ 0\ 0\ 0\ 0\ 0]$, $\theta_1=[0\ 0\ 1\ 0\ 0\ 1\ 0\ 1\ 0.95\ 0\ 0\ 0\ 0\ 0\ 0\ 0\ 0\ 0\ 0]$.

When $g = 2$, the results are: $\delta_2=[0\ 0\ 0.95\ 0\ 0\ 0\ 0\ 0\ 0\ 0\ 0\ 0\ 0]$, $\theta_2=[0\ 0\ 0\ 0\ 0\ 0\ 0\ 0\ 0\ 0\ 0\ 0\ 0.9025\ 0\ 0\ 0\ 0\ 0\ 0\ 0]$.

When $g = 3$, we get: $\delta_3=[0\ 0\ 0\ 0\ 0\ 0\ 0\ 0\ 0\ 0\ 0\ 0]$.

Thus, the termination condition is satisfied and the reasoning results, i.e., the fuzzy truth values, 0.9025, 0, 0, 0, 0, 0, 0, 0, 0 and 0, from the output neurons $\sigma_{11}, \dots, \sigma_{20}$, are obtained, respectively. Because the value 0.9025 is the highest fuzzy truth values among all values from output neurons, the proposition “ A_g ” corresponding to σ_{11} is satisfied. That is to say, the fault type is A_g .

Case 2: The fault is of type AB_g .

Similarly, we obtain wavelet singular values, 12.2845, 14.6508, 0.1033 and 2.4165, for S_a, S_b, S_c and S_0 , respectively. The normalized feature values of s_a, s_b, s_c and s_0 are 0.8385, 1, 0.0071 and 0.1649, respectively.

Thus, the initial parameter matrices of the rFRSNPS for fault classification are: $\theta_0=[1\ 0\ 1\ 0\ 0\ 1\ 0\ 0\ 0\ 0\ 0\ 0\ 0\ 0\ 0\ 0\ 0\ 0\ 0\ 0]$, $\delta_0=[0\ 0\ 0\ 0\ 0\ 0\ 0\ 0\ 0\ 0\ 0\ 0\ 0]$, $C=[0.95\ 0.95\ 0.95\ 0.95\ 0.95\ 0.95\ 0.95\ 0.95\ 0.95\ 0.95]$.

When $g = 1$, we get: $\delta_1=[1\ 0\ 0\ 0\ 0\ 0\ 0\ 0\ 0\ 0\ 0\ 0\ 0]$, $\theta_1=[0\ 0\ 1\ 0\ 1\ 0\ 0\ 1\ 0.95\ 0\ 0\ 0\ 0\ 0\ 0\ 0\ 0\ 0\ 0]$.

When $g = 2$, we get: $\delta_2=[0\ 0\ 0\ 0\ 0\ 0.95\ 0\ 0\ 0\ 0\ 0\ 0]$, $\theta_2=[0\ 0\ 0\ 0\ 0\ 0\ 0\ 0\ 0\ 0\ 0\ 0\ 0\ 0.9025\ 0\ 0\ 0\ 0\ 0\ 0]$.

When $g = 3$, we get: $\delta_3=[0\ 0\ 0\ 0\ 0\ 0\ 0\ 0\ 0\ 0\ 0\ 0]$.

Thus, the termination condition is satisfied and the reasoning results, i.e., the fuzzy truth values, 0, 0, 0, 0.9025, 0, 0, 0, 0, 0 and 0, from output neurons $\sigma_{11}, \dots, \sigma_{20}$, are obtained, respectively. Because the value 0.9025 is the highest fuzzy truth values among all values from output neurons, the proposition “ AB_g ” corresponding to σ_{14} is satisfied. That is to say, the fault type is AB_g .

Case 3: The fault is of type AB .

Likewise, wavelet singular values, 10.6887, 10.6888, $5.4415e^{-4}$ and $2.6927e^{-14}$, are obtained for S_a, S_b, S_c and S_0 , respectively. The normalized feature values of s_a, s_b, s_c and s_0 are 1, 1, 0 and 0, respectively.

Thus, the initial parameter matrices of the rFRSNPS for fault classification are: $\theta_0=[0\ 1\ 1\ 0\ 1\ 0\ 0\ 1\ 0\ 0\ 0\ 0\ 0\ 0\ 0\ 0\ 0\ 0\ 0\ 0]$, $\delta_0=[0\ 0\ 0\ 0\ 0\ 0\ 0\ 0\ 0\ 0\ 0\ 0]$, $C=[0.95\ 0.95\ 0.95\ 0.95\ 0.95\ 0.95\ 0.95\ 0.95\ 0.95\ 0.95]$.

When $g = 1$, we get: $\delta_1=[0\ 1\ 0\ 0\ 0\ 0\ 0\ 0\ 0\ 0\ 0\ 0]$, $\theta_1=[0\ 0\ 1\ 0\ 1\ 0\ 0\ 1\ 0.95\ 0\ 0\ 0\ 0\ 0\ 0\ 0\ 0\ 0\ 0]$.

When $g = 2$, we get: $\delta_2=[0\ 0\ 0\ 0\ 0\ 0\ 0\ 0.95\ 0\ 0\ 0]$, $\theta_2=[0\ 0\ 0\ 0\ 0\ 0\ 0\ 0\ 0\ 0\ 0\ 0\ 0\ 0\ 0\ 0\ 0\ 0\ 0\ 0.9025\ 0\ 0\ 0]$.

When $g = 3$, we get: $\delta_3=[0\ 0\ 0\ 0\ 0\ 0\ 0\ 0\ 0\ 0\ 0]$.

Thus, the termination condition is satisfied and the reasoning results, i.e., the fuzzy truth values, 0, 0, 0, 0, 0, 0, 0.9025, 0, 0 and 0, from output neurons $\sigma_{11}, \dots, \sigma_{20}$, are obtained, respectively. Because the value 0.95 is the highest fuzzy truth values among all values from output neurons, the proposition “*AB*” corresponding to σ_{17} is satisfied. That is to say, the fault type is *AB*.

Case 4: The fault is of type ABC.

Similarly, wavelet singular values, 8.7031, 4.4449, 7.6964 and $1.2640e^{-14}$, are achieved for S_a, S_b, S_c and S_0 , respectively. The normalized feature values of s_a, s_b, s_c and s_0 are 1, 0.5107, 0.8843 and 0, respectively.

Thus, the initial parameter matrices of the rFRSNPS for fault classification are: $\theta_0=[0 \ 1 \ 1 \ 0 \ 1 \ 0 \ 0 \ 0 \ 0 \ 0 \ 0 \ 0 \ 0 \ 0 \ 0 \ 0 \ 0 \ 0 \ 0 \ 0 \ 0 \ 0]$, $\delta_0=[0 \ 0]$, $C=[0.95 \ 0.95]$.

When $g = 1$, we get: $\delta_1=[0 \ 1 \ 0]$, $\theta_1=[0 \ 0 \ 1 \ 0 \ 1 \ 0 \ 1 \ 0 \ 0 \ 0.95 \ 0 \ 0 \ 0 \ 0 \ 0 \ 0 \ 0 \ 0 \ 0 \ 0 \ 0]$.

When $g = 2$, we get: $\delta_2=[0 \ 0 \ 0 \ 0 \ 0 \ 0 \ 0 \ 0 \ 0 \ 0 \ 0 \ 0 \ 0.95 \ 0 \ 0 \ 0 \ 0 \ 0 \ 0 \ 0 \ 0 \ 0 \ 0]$, $\theta_2=[0 \ 0]$.

When $g = 3$, we get: $\delta_3=[0 \ 0]$.

Thus, the termination condition is satisfied and the reasoning results, i.e., the fuzzy truth values, 0, 0, 0, 0, 0, 0, 0, 0, 0 and 0.9025, from output neurons $\sigma_{11}, \dots, \sigma_{20}$, are gained, respectively. Because the value 0.95 is the highest fuzzy truth values among all values from output neurons, the proposition “*ABC*” corresponding to σ_{20} is satisfied. That is to say, the fault type is *ABC*.

According to the classification processes described above, the testing results for various values of fault resistance and various fault locations, and various fault inception angles are shown in Tables 2. In summary, the classification results of 1200 simulations is shown in Table 3. It can be seen that the method presented in this paper achieves good results with high accuracy, and is immune to various fault conditions, such as fault resistance, fault locations and fault inception angles.

6. Robustness to Transmission Line Parameters and Noise

In this section, we will discuss the robustness of the introduced approach to transmission line parameters and noise.

To test the effect of different transmission line parameters on the accuracy of the presented approach, two different transmission lines are used to produce 100 testing samples. The parameter values are listed as follows. The length, voltage, positive-sequence impedance, zero-sequence impedance, positive-sequence capacitance and zero-sequence capacitance in two transmission lines are 150 km, 500 kV, $3.69+j55.2 \ \Omega$, $32.7+j230 \ \Omega$, $13.3 \ nF/km$, $8.77 \ nF/km$, and 250 km, 500 kV, $3.97+j38.9 \ \Omega$, $32.8+j239 \ \Omega$, $18.0 \ nF/km$ and $7.15 \ nF/km$, respectively. The classification results are shown in Table 4. It can be seen that the accuracy is 100% even when transmission lines change. In other words, the proposed approach in this paper is robust to transmission line parameters.

Let us examine now the effect of measurement noise (e.g., it could be caused by the measurement errors in meters) on the accuracy of the proposed approach. Assume that the

Table 2: **Results of fault classification for various fault conditions.** FIA, FauR and FauL denote fault inception angles, fault resistance and fault locations, respectively

Fault conditions	s_a	s_b	s_c	s_0	Fault type/Probability	
FIA	0°	1	0.0544	0.0424	0.3488	$A_g/0.9025$
	30°	1	0.0936	0.0894	0.3684	$A_g/0.9025$
	60°	1	0.1139	0.1188	0.3774	$A_g/0.9025$
	90°	1	0.1372	0.1569	0.3660	$A_g/0.9025$
	120°	1	0.1716	0.1777	0.3719	$A_g/0.9025$
	150°	1	0.2293	0.2046	0.3752	$A_g/0.8572$
FauR	0Ω	0.9092	1	0.0505	0.2815	$AB_g/0.9025$
	50Ω	0.5375	1	0.0787	0.2376	$AB_g/0.9025$
	100Ω	0.4505	1	0.0915	0.3023	$AB_g/0.7933$
	200Ω	0.4252	1	0.01204	0.2972	$AB_g/0.7132$
FauL	0km	1	0.9442	0.0630	$2.442e^{-14}$	$AB/0.9025$
	50km	1	0.8980	0.1199	$3.558e^{-14}$	$AB/0.9025$
	100km	1	0.9004	0.1126	$3.523e^{-14}$	$AB/0.9025$
	150km	1	0.8961	0.1116	$3.912e^{-14}$	$AB/0.9025$
	200km	1	0.8994	0.1036	$2.993e^{-14}$	$AB/0.9025$

Table 3: **Classification results of 1200 independent simulations.** NoS and NoIFC represent the number of samples and the number of incorrect fault classification, respectively

Fault types		NoS	NoIFC	Accuracy
single-phase-to-ground fault	A_g	120	0	100%
	B_g	120	0	100%
	C_g	120	0	100%
Double-phase-to-ground fault	AB_g	120	0	100%
	BC_g	120	0	100%
	CA_g	120	0	100%
Phase-to-phase fault	AB	120	0	100%
	BC	120	0	100%
	CA	120	0	100%
Three phase fault	ABC	120	0	100%
Total		1200	0	100%

Table 4: **Classification results for different parameter values**

Lines	Number of samples	Number of incorrect classifications	Accuracy
1	120	0	100%
2	120	0	100%

wavelet singular values are obtained from the currents with Gaussian white noise having different signal-to-noise rates (SNR), 40 dB, 30 dB and 20 dB. For each case, 100 independent samples are used to test the accuracy. The final results are listed in Table 5. It can be seen that the classification accuracy is 98% even when SNR is 20dB. Meanwhile, classification accuracy of other methods with the presence of noise is also shown in Table 5, where the

Table 5: Classification results for different SNR

SNR (dB)	Number of samples	Number of incorrect classifications	Classification accuracy		
			Method in this paper	Method in [24]	Method in [19]
40	100	0	100%	100%	100%
30	100	0	100%	93.94%	99.4%
25	100	0	100%	–	–
20	100	2	98%	–	–
15	100	12	88%	–	–
10	100	28	72%	–	–

symbol ‘–’ means that this case was not considered in the corresponding reference. From Table 5, we can see that when SNR is greater than or equal to 20 dB, the proposed approach is superior to the benchmark methods considered with respect to robustness to noise.

7. Conclusions

This study presented a novel approach combining wavelet transform, singular value decomposition and fuzzy reasoning spiking neural P systems to classify ten types of short-circuit faults occurring in power system transmission lines. This approach consists of feature extraction of fault currents and classification models. Several cases considering various fault inception angles, various fault resistance and various fault locations were used to carry out the experiments to show the feasibility, effectiveness and robustness to parameters and noise of the introduced approach. Following this work, more and complex fault situations in power systems such as double-circuit transmission lines and transmission line with series capacitors will be considered in the future study.

Acknowledgements. This work is partially supported by the Fundamental Research Funds for the Central Universities (A0920502051619-36), the National Natural Science Foundation of China (61373047, 61672437), and the Research Project of Key Laboratory of Fluid and Power Machinery (Xihua University), Ministry of Education, P.R. China (JYBFXQ-1).

References

- [1] Păun, Gh., Rozenberg, G., Salomaa A. (Eds.): The Oxford Handbook of Membrane Computing, Oxford University Press, 2010.
- [2] Song, T., Pan, L.Q., Păun, Gh.: Asynchronous Spiking Neural P Systems with Local Synchronization. *Information Sciences* 219, 197–207 (2013).
- [3] Zeng, X., Zhang, X., Song, T., Pan, L.: Spiking Neural P Systems with Thresholds, *Neural Computation* 26, 1340–1361 (2014).
- [4] Zhang, X., Zeng, X., Luo, B., Pan, L.: On Some Classes of Sequential Spiking Neural P Systems, *Neural Computation* 26, 974–997 (2014).
- [5] Zhang, G., Cheng, J., Wang, T., Wang, X., Zhu, J.: *Membrane Computing: Theory & Applications*, Science Press, Beijing, China, 2015.

- [6] Zhang, G., Gheorghe, M., Pan, L., Pérez-Jiménez, M.J.: Evolutionary Membrane Computing: a Comprehensive Survey and New Results. *Information Sciences* 279, 528–551 (2014).
- [7] Zhang, G., Cheng, J., Gheorghe, M., Meng, Q.: A Hybrid Approach Based on Differential Evolution and Tissue Membrane Systems for Solving Constrained Manufacturing Parameter Optimization Problems. *Applied Soft Computing* 13(3), 1528–1542 (2013).
- [8] Ciobanu, G., Păun, Gh., Pérez-Jiménez, M.J. (Eds.): *Applications of Membrane Computing*. Springer-Verlag, Berlin, 2006.
- [9] Frisco, P., Gheorghe, M., Pérez-Jiménez, M.J. (Eds.): *Applications of Membrane Computing in Systems and Synthetic Biology*. Springer-Verlag, Berlin, 2014.
- [10] Zhang, G., Rong, H., Neri, F., Pérez-Jiménez, M.J.: An Optimization Spiking Neural P system for Approximately Solving Combinatorial Optimization Problems. *International Journal of Neural Systems*, 24(5), 1440006 (16 pages) (2014)
- [11] Wang, J., Shi, P., Peng, H., Pérez-Jiménez, M.J., Wang, T.: Weighted Fuzzy Spiking Neural P Systems. *IEEE Transactions on Fuzzy Systems* 21(2), 209-220 (2013)
- [12] Wang, T., Zhang, G.X., Pérez-Jiménez, M.J.: Fuzzy Membrane Computing: Theory and Applications. *International Journal of Computers, Communications & Control* 10(6), 904-935 (2015).
- [13] Wang, T., Zhang, G.X., Zhao, J.B., He, Z.Y., Wang, J., Pérez-Jiménez, M.J.: Fault Diagnosis of Electric Power Systems Based on Fuzzy Reasoning Spiking Neural P Systems. *IEEE Transactions on Power Systems*, 30(3), 1182-1194 (2015)
- [14] Peng, H., Wang, J., Pérez-Jiménez, M.J., Wang, H., Shao, J., Wang, T.: Fuzzy Reasoning Spiking Neural P System for Fault Diagnosis. *Information Sciences*, 235(20), 106-116 (2013)
- [15] Silva, K.M., Souza, B.A., Brito, N.S.D.: Fault Detection and Classification in Transmission Lines Based on Wavelet Transform and ANN. *IEEE Transactions on Power Delivery*, 21(4), 2058-2063 (2006)
- [16] He, Z.Y., Fu, L., Lin, S., Bo, Z.Q.: Fault Detection and Classification in EHV Transmission Line Based on Wavelet Singular Entropy. *IEEE Transactions on Power Delivery*, 25(4), 2156-2163 (2010)
- [17] Youssef, O.A.S.: Combined Fuzzy-Logic Wavelet-based Fault Classification Technique for Power System Relaying. *IEEE Transactions on Power Delivery*, 19(2), 582-589 (2004)
- [18] Li, D.M., Liu, Z.G., Su, Y.X., Cai, J.: Fault Recognition Based on Multi-Wavelet Packet and Artificial Network. *Electric Power Automation Equipment*, 29(1), 99-103 (2009)
- [19] Yang, J.W., He, Z.Y.: Study on Recognition of Fault Transients Using Hybrid Fuzzy Petri Net. *Power System Technology*, 36(2), 250-256 (2012)
- [20] Bo, Z.Q., Agganval, R.K., Johns, A.T, Yu, H., Song, Y.H.: A New Approach to Phase Selection Using Fault Generated High Frequency Noise and Neural Networks. *IEEE Transactions on Power Delivery* 12(1), 106–115, (1997).
- [21] Suonan, J.L., Zhang, J.K., Liu, H., et al.: A New Method for Fault Components Extraction and Fault Phases Selection. *Automation of Electric Power Systems*, 27(16), 58-61 (2003)
- [22] Mallat, S.G.: A Theory for Multiresolution Signal Decomposition: the Wavelet Representation. *IEEE Transactions on Pattern Analysis and Machine Intelligence*, 11(7), 674-693 (1989)
- [23] Hou, Z.J.: Adaptive Singular Value Decomposition in Wavelet Domain for Image Denoising. *Pattern Recognition*, 36(8), 1747-1763 (2003)
- [24] Lin, S., He, Z.Y., Zang, T.L., Qian, Q.Q.: Novel Approach of Fault Type Classification in Transmission Lines Based on Rough Membership Neural Networks. *Proceeding of the CSEE*, 30(28), 72-79 (2010)